Available online at www.sciencedirect.com
SCIENCE DIRECT
Carbohydrate Polymers 60 (2005) 363–378
Carbohydrate Polymers
www.elsevier.com/locate/carbpol

Swelling, mechanical properties and effect of annealing of scleroglucan gels

Einar Aasprong[a], Olav Smidsrød[a], Bjørn Torger Stokke[b,*]

[a]Norwegian Biopolymer Laboratory, Department of Biotechnology, The Norwegian University of Science and Technology, NTNU, NO-7491 Trondheim, Norway
[b]Norwegian Biopolymer Laboratory, Department of Physics, The Norwegian University of Science and Technology, NTNU, NO-7491 Trondheim, Norway

Received 19 August 2003; revised 17 October 2003; accepted 3 December 2003
Available online 7 April 2005

Abstract

Scleroglucan gels were made by alkaline denaturation and subsequent renaturation of the scleroglucan triple helix by in situ neutralization. Gels prepared from 4 to 5% scleroglucan solutions were incubated in aqueous solutions and dependence of pH, temperature and ionic strength, I, were studied. (i) The scleroglucan gels were observed to be stable for more than 600 days in solutions of NaCl or $CaCl_2$ ($I \in 0$–3 M) or in solutions of pH $\in$ 1–12 ($I = 0.1$ M) at ambient temperatures. Gels incubated at pH 13 were found to dissolve within 1 day of storage. (ii) Under conditions, where a triple helical conformation of scleroglucan prevails, isotropic swelling was observed. This was consistent with a weakly negatively charged network, and a charge density of 0.017 per tetramer repeating unit of the scleroglucan was determined using counter-ion binding. (iii) Annealing in aqueous 0.1 M NaCl at 96 °C for 5 h yielded a marked increase in the failure strain and stress. Gels subsequently transferred to incubation at 21 °C maintained their acquired properties for more than 400 days. (iv) Large deformation data in uniaxial compression were adequately fitted by a model consisting of a linear and an exponential regime, with two material parameters, the Young's modulus (E) and a transition strain (ε_t) between the two regimes.
© 2005 Elsevier Ltd. All rights reserved.

Keywords: Scleroglucan; (1→3)-β-Glucan; Gels; Stability; Mechanical properties; Annealing; Large deformation; Stress–strain

1. Introduction

The polysaccharide scleroglucan consists of a (1→3)-β-D-glucan backbone branched with one (1→6)-β-D-glucose residue at every third glucose unit of the backbone (Johnson et al., 1963). The polysaccharides of this structure with various degree of branching are commonly known as β-1,3-glucans. Examples of these are schizophyllan, laminaran, lentinan, cinerean and the unbranched linear curdlan.

Common for curdlan and the comblike (1→6)-β-D-gluco-(1→3)-β-D-glucans is that high molecular weight samples adopt a triple helical structure that is preserved in aqueous solution (Bluhm, Deslandes, & Marchessault, 1982). The comblike-branched (1→3)-β-D-glucans have increased water solubility compared to the linear curdlan.

The triple helical conformation of scleroglucan is very stiff, with a persistence length (L_{pe}) of approximately 150 nm at room temperature (Carriere, Amis, Schrag, & Ferry, 1985; Stokke & Brant, 1990; Yanaki, Norisuye, & Fujita, 1980). In neutral aqueous solution a temperature dependent conformational transition between two triple helical conformational states has been reported. Above the melting temperature (T_M) of about 6 °C, triple-helix II prevails and below T_M, triple-helix I prevails (Itou, Teramoto, Matsua, & Suga, 1986, 1987; Kitamura & Kuge, 1989). At alkaline conditions an increase in this melting temperature is observed (Bo, Milas, & Rinaudo, 1987).

Destabilizing the triple helical conformation induces strand separation to a more flexible single stranded conformation. The triple helical conformation can be destabilized in neutral aqueous solution by a reduction of molecular weight to less than $M_w = 5 \times 10^4$ g mol^{-1} (Kojima, Tabata, Itoh, & Yanaki, 1986) or by an increase in temperature to above $T = 135$ °C for high molecular weight samples (Yanaki, Tabata, & Kojima, 1985).

* Corresponding author. Tel.: +47 73 59 34 34; fax: +47 73 59 77 10.
E-mail address: bjorn.stokke@phys.ntnu.no (B.T. Stokke).

0144-8617/$ - see front matter © 2005 Elsevier Ltd. All rights reserved.
doi:10.1016/j.carbpol.2005.01.016

A concentration of OH^- above 0.1 M in aqueous solution (Bo et al., 1987) or a change in solute composition, i.e. in the binary solute of dimethylsulfoxide/water to a water weight fraction, $W_H < 0.13$ (Sato, Norisuye, & Fujita, 1981) will also destabilize the triple helical conformation.

The transition to a single stranded state and the subsequent reversion to conditions favoring a triple-helical state are often referred to as denaturation and renaturation, respectively. Denaturation–renaturation yields a mixture of linear and macrocyclic topologies and multi-chain clusters with relative abundance mainly determined by the polymer concentration and chain length (Falch, Elgsaeter, & Stokke, 1999; Stokke, Elgsaeter, & Kitamura, 1993). Subsequent annealing may alter the relative distribution of species following renaturation (Falch & Stokke, 2001; Kitamura et al., 1996).

For concentrated solutions ($c > 1.5\%$) renaturation gels may be formed by neutralization of the alkaline solution (Aasprong, Smidsrød, & Stokke, 2003). Gels from curdlan, the unbranched analogue of scleroglucan, is also reported to be formed by heat treatment or by neutralization of the alkaline solution (Konno & Harada, 1991). Due to the common triple-helical backbone arrangement, these polysaccharides may be expected to share some common features while differences are expected to result from the branching of the scleroglucan. The gelation mechanism of curdlan including the effect of time-dependent annealing has recently been studied by Zhang, Nishinari, Williams, Foster, and Norton (2002).

The triple helical structure is also a basis for the increased stability of the polysaccharide towards thermal and chemical degradation as compared to single stranded chains (Hjerde, Stokke, Smidsrød, & Christensen, 1998). Due to the thermal stability of scleroglucan (Kalpacki, Jeans, Magri, & Padolewski, 1990), selective placement of scleroglucan gels in oil reservoirs for permeability control of injected water and resulting enhanced oil production is one possible application. The (1→6)-β-D-gluco-(1→3)-β-D-glucans are also of interest for biomedical applications due to their functions as biological response modifiers (Bohn & BeMiller, 1995; Wasser, 2002).

The aim of the present work is to further study the scleroglucan renaturation gels (Aasprong et al., 2003) and the time dependence of their physical properties when incubated in aqueous solutions. The triple helical motif of scleroglucan in aqueous solution is of major importance also for the gels of this study and central parameters will be those previously described which are known to influence the stability of this triplex.

Within the conformational region of the triple-helix II, incubation in neutral aqueous solution at 21 °C was examined. Close to the borders of the triple-helix II region in neutral aqueous solution, the temperatures 6 and 96 °C were chosen. Incubation at 6 °C is on the border between the two triple helical conformations. Incubation at 96 °C is within the triple-helix II region approaching the transitional zone to the single strand conformation for the high molecular sample (Kitamura & Kuge, 1989). The variation of pH's of the incubation solutions covered the range from acidic conditions (pH 1) to alkaline conditions (pH 13). Solutions of Ca^{2+} were included as well as solutions of Na^+ when exploring the gels dependence of the ionic strength of the incubation solutions. Studying the long-term stability of the gels was of interest with respect to possible applications, but also with respect to comparison with the reported thermal stability of the scleroglucan solution. Finally, it was of interest to extend the studies, previously performed on the effect of annealing of scleroglucan in dilute aqueous solutions (Falch & Stokke, 2001), to include the high concentration regime.

2. Materials and methods

2.1. Samples

The scleroglucan used was Actigum CS11 provided by Sanofi Bioindustries, France. The elemental composition (C, N and S) % (w/w) of the dried powder was analyzed using a Carlo Erba, Milan, Italy (Kirsten, 1979) and found to be carbon (43.5%), nitrogen (<0.1%) and sulfur (not detected). The CS11 sample was found to contain 0.041 negatively charged groups per repeating unit of the scleroglucan. All reagents used were p.a. grade and all water was double distilled, de-ionized Milli-Q water (MQ).

2.2. Gel preparation

Gels were prepared by the procedure described by Aasprong et al. (2003). Scleroglucan solutions were prepared by adding powdered scleroglucan to aqueous 0.316 M NaOH under continuous stirring. The solution was stirred for 4–5 h at room temperature and controlled for visual homogeneity. A 15 min degassing was performed before adding formamide (methanoic amide) to a final concentration of 0.632 M. After mixing, the solution was filled in cylinders ($d_0 = 20$ mm, $l_0 = 8.0$ mm) and given an airtight sealing. The samples were kept dark at room temperature for 1 week. If otherwise not stated the gels were molded from 5% scleroglucan solutions. The measured dry weight of the gels used for determination of the gel network charge indicated that the loss of scleroglucan during extended washing of the gels might be as high as 40% of the starting material.

In the case of gels subsequently annealed at 96 °C the experimental setup used for rheological characterization reached the limit of the maximum loading force of the apparatus. Thus, parallel experiments were performed using gels with a reduced surface area ($d_0 = 10.3$ mm, $l_0 = 19.5$ mm) molded from a 4% scleroglucan solution. These gels were sliced in three parts ($d_0 = 10.3$ mm, $l_0 \approx 6.5$ mm) before measuring.

2.3. Determination of the sample- and gel-network charge

Gels were prepared according to the procedure described above. Using Mg^{2+} as the counter ion, the degree of negative charge of the starting material and the gel network was determined. Aliquots of 10 mL, 5% scleroglucan solutions were dialyzed against 3×6 L of 0.1 M NaCl, 3×6 L of MQ-water, 3×6 L of 0.5 M $MgCl_2$, 13×6 L of MQ-water and finally 70 mL of 0.125 M HCl. Aliquots of the same sample volume of MQ-water were employed as blanks. The amount of Mg^{2+}-binding was determined by atomic absorption employing a Perkin Elmer 560 Atom Absorption spectrometer equipped with a Ca–Mg Intesitron lamp. The Mg^{2+}-binding to the dialysis membrane was determined separately and subtracted from the total determined amount of Mg^{2+} bound in the system. The use of a membrane was not necessary for the equilibration of the gels. A degree of negative charge (D_c) of 0.041 per repeating unit was found for the scleroglucan, CS11. Stokke, Elgsaeter, Smidsrød, and Christensen (1995) reported a $D_c=0.045$ for CS11, not taking into account the Mg^{2+} bound to the dialysis membrane. In the present study, this accounted for approximately 10% of the total. As part of their study of a crosslinked system of a scleroglucan derivative, Coviello, Grassi, Rambone, and Alhaique (2001) reported the IR spectra of the CS11 sample of scleroglucan and the corresponding polycarboxylated derivative (sclerox). For the sclerox sample, they assign the carboxyl groups to 1623.4 cm^{-1}. An unassigned top in proximity to this is also apparent in the IR spectrum of the CS11 starting material. In this region of the IR spectrum no fundamental band would be expected for a pure glucan sample (Mohaček-Grosev, Božac, & Puppels, 2001), except perhaps for the bending of bound water.

For the scleroglucan renaturation gels $D_c=0.017$ was found. Gelation by dialysis of the alkaline solution (0.316 M NaOH) of scleroglucan (5%) against 0.1 M HCl yielded $D_c=0.014$. Storing the alkaline solution at 80 °C for 40 min prior to dialysis made no significant difference ($D_c=0.017$). Scleroglucan gels prepared by dialysis of the DMSO-solution against MQ-water was determined to $D_c=0.028$.

As a potential source of negatively charged groups the amount of protein present in the system and released under varying conditions of dialysis was estimated using the Folin phenol protein quantitation method of Lowry, Rosebrough, Farr, and Randall (1951). The carbohydrate concentration was determined by the Phenol sulfuric acid method of Dubois, Gilles, Hamilton, Rebers, and Smith (1956). For all solutions the polysaccharide concentrations were tolerable low with respect to reliable protein determination (Peterson, 1979). Using a BSA-standard the CS11-sample was found to contain 0.46% (w/w) protein. Using a 5% solution of scleroglucan the released amount of carbohydrate and protein during dialysis was examined (Table 1(a)). During dialysis of a 5% scleroglucan sample, kept at 80 °C for 40 min before dialyzing against 0.1 M HCl, 0.26% (w_{prot}/w_{tot}) of protein as related to the initial total weight of the sample, was released. Reversed phase HPLC by precolumn fluorescence derivatization with *o*-phthaldialdehyde, using a NovaPak C18 cartridge (Waters, Milford, MA, USA) was used for amino acid analysis according to the method of Lindroth and Mopper (1979) as modified by Flynn (1988). The dialyzate was found free of amino acids. After acid hydrolysis (6 M HCl, 2 days) a content of 0.03% (w_{prot}/w_{tot}) of protein, in the form of free amino acids, was detected. The two negatively charged amino acids, aspartic and glutamic acid, were each found to comprise 1/4 of this. The yield of released protein, though significantly lower than that found by the method of Lowry (Table 1(b)), equaled the total amount of protein found to be present in the sample by Palace and Phoebe (1997).

Table 1(a)
Release of carbohydrate and protein following dialysis [% (w/w)]

Solvent	Dialysis solution	$[Glucose]_{released}/[Glucose]_0$	$[Protein]_{released}/[Protein]_0$
H_2O	H_2O	<0.5	0
H_2O	0.1 M HCl	<0.5	25
DMSO	H_2O	2.5	5
0.316 M NaOH	0.1 M HCl	2–2.5	20–55

2.4. Incubation procedure

After molding, all gels were first washed in 3×6 L of aqueous 0.1 M NaCl at 6 °C, in dark. Gels to be stored in aqueous solutions containing NaCl or $CaCl_2$ at 6 and 21 °C were washed in 3×6 L of incubation solution at incubation temperature and in dark. Other gels were incubated directly in excess of incubation solution. The incubation solutions of pH 2 and 12 were adjusted to the same ionic strength as the pH 1 and 13 solutions ($I=0.1$ M) using NaCl. The incubation solutions were purged for 5 min with N_2 prior to use. The storage containers were sealed and placed in dark at temperatures 6±2, 21±2 and 96±2 °C.

A short notation ($SclGel_T$ [temperature], [concentration] M [salt], (t=[time])) is used for describing the incubation conditions and duration. As an example, the notation $SclGel_{T6,\ 0.1\ M\ NaCl,\ (t=346\ days)}$ denotes a gel stored in a 0.1 M NaCl solution at 6 °C for 346 days. For samples stored at a given pH, this is also given in the subscript. Gels incubated in solutions containing formaldehyde (250–1000 ppm) showed the same time dependence as those incubated

Table 1(b)
Protein levels in scleroglucan and release of protein from a 5% scleroglucan sample, kept at 80 °C for 40 min dialyzed against 0.1 M HCl [w_{prot}/w_{tot}%]

Method of analysis/ reference	Folin phenol method	Acid hydrolysis/ HPLC	Palace and Phoebe (1997)
Protein present in sample	0.46		0.034
Protein released through dialysis	0.26	0.03	

without formaldehyde under conditions where microbial degradation was not encountered.

2.5. Rheological investigations

The gels were transferred from the storage solution to a large volume of the same solution at room temperature. Gels annealed at 96 °C were equilibrated for 1 h at room temperature, while gels stored at 6 °C were left over night before determining their properties. The gel diameter was determined using a slide caliper. No asymmetry was observed for the circular circumference of the end surfaces, for any of the studied gel cylinders. The average value of two orthogonal measurements of the diameter was used for calculating the surface area. Stress–strain measurements were carried out at room temperature using a Stable Micro Systems, Texture Analyser (XT2), measuring force versus axial deformation distance of the gel at deformation rate, $\Delta l/\Delta t = 0.1$ mm s^{-1}. The trigger value for the detection of the gel surface was set to a measured force of 0.01 N and the distance from the sample board at the trigger point was taken as the gel height ($l_{\varepsilon=0}$) in the unstrained state, were ε is the strain. An example of a measured gel ($l_{\varepsilon=0}$ = 8.29 mm) is given in Fig. 1. No barreling of the gels was observed during deformation. For some of the gels, a significant change in volume and hence in the polymer concentration, was observed following storage. The presented values are those of the measured gels without recalculating the parameters to a common reference volume or concentration.

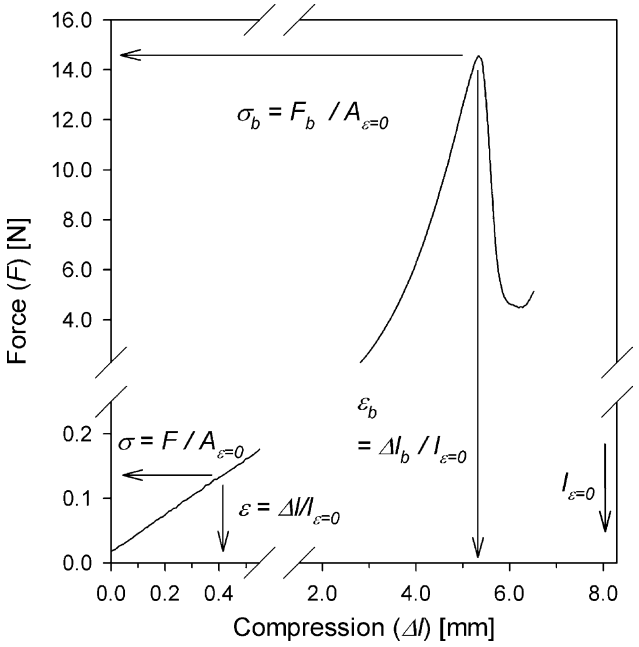

Fig. 1. Compression deformation of a gel of height ($l_{\varepsilon=0}$ = 8.29 mm). The initial gradient from $\varepsilon = 0$ to -0.05 was used for calculating Young's modulus (E). The nominal strain and stress at failure are given as ε_b and σ_b, respectively.

2.6. Large deformation models

An idealized relation between stress and strain for the purely entropic network as derived from the Gaussian statistical theory of rubber elasticity (Treloar, 1975) is:

$$\bar{\sigma} = \frac{E}{3}\left(\lambda^2 - \frac{1}{\lambda}\right) \tag{1}$$

The nominal stress is given by the force (F) acting on the initial surface area ($A_{\varepsilon=0}$) of the unstrained sample ($\sigma = F/A_{\varepsilon=0}$). The bar over σ denotes true stress as related to the actual surface area ($\bar{\sigma} = F/A$) of the strained sample. E is the Young's modulus, λ ($=1+\varepsilon$) is the extension ratio and ε is the strain.

A significant enthalpic contribution to the elasticity and hence a deviation from Eq. (1) may be expected for biopolymer gels. Clark and Ross-Murphy (1987) and Ferry (1980) reviewed approaches to deal with large deformation of biopolymer gels. Blatz, Sharda, and Tschoegl (1974) give one such model (the BST equation). They proposed a strain energy density function that in its simplest form yields the following expression for simple tension:

$$\bar{\sigma} = \frac{2E}{3n}(\lambda^n - \lambda^{-n/2}) \tag{2}$$

with n being a material constant which for ideal rubber elasticity equals 2. The BST-equation as stated in Eq. (2) allows for gross deviations from Eq. (1) (Clark & Ross-Murphy, 1987). The expanded expression of Blatz et al. including two additional material constants yields satisfactory fit of data at deformations higher than what Eq. (2) can handle. Still, for gelatin gels the BST-equation, as stated in Eq. (2), was found to describe large deformation rheological experiments adequately both in shear deformation and in compression (Bot, van Amerongen, Groot, Hoekstra, & Agterof, 1996). In a section of their paper Groot, Bot, and Agterof (1996) give a brief review of the BST-model and interpret the parameters. Both the gelatin gels and the scleroglucan renaturation gels are made by denaturation and subsequent renaturation of biopolymers, which in their native states exist as rigid triple helixes. In this context, it is of interest to test whether the BST-equation adequately describes deformation of scleroglucan renaturation gels.

One other method applied to large deformation experiment data will be presented below. Fung (1967) derived mathematical formulations for describing elasticity of soft tissues in simple elongation. The elasticity of living soft tissues is strongly nonlinear and the expressions derived by Fung are exponential ones. The simplest expression is obtained from the following relation:

$$\frac{d\sigma}{d\lambda} = \alpha\sigma \quad (1 \le \lambda \le \lambda_y) \tag{3}$$

where λ_y is the upper limit of validity of the exponential stress–strain relationship, and α is a constant. Integration of Eq. (3) yields:

$$\sigma = \frac{1}{c}\, e^{\alpha\lambda} \tag{4}$$

where c is an integration constant. The boundary condition $\sigma=\sigma^*$ at $\lambda=\lambda^*$, is sufficient to determine the integration constant, yielding

$$\bar{\sigma} = \sigma^* \lambda\, e^{\alpha(\lambda-\lambda^*)} \tag{5}$$

Although one can choose any point (σ^*, λ^*) on the stress–strain curve, Fung recommended to chose σ^* and λ^* at a point which may be judged particularly significant from the point of view of physiology. The strain energy per unit volume of the undeformed tissue is given

$$W(\lambda) = \frac{1}{c\alpha}[e^{\alpha\lambda} - e^{\alpha}] \quad (1 \le \lambda \le \lambda_y) \tag{6}$$

Since Fung's contribution (1967) there has been considerable awareness to nonlinear, exponential stress–strain relation within biological materials. This has, however, not been the case for biopolymer gels.

Our experimental data suggest there is a continuous transition from an initial linear stress–strain regime (σ_l) to an exponential stress–strain regime (σ_e) (in the nominal stress) during uniaxial compression. According to Ferry (1980), Eq. (1) does not hold closely above extensions of about 20%. For low values of $|\varepsilon|$ Eq. (1) reduces to Hooke's law (Eq. (7)). With increasing strain ($|\varepsilon|$) the difference between Eqs. (1) and (7) will increase, but even at $|\varepsilon|=0.2$, they differ by less than 2%. Although the data suggesting a similar relation in uniaxial tension, is limited in this study, the set of equations is expressed as to be valid for both forms of deformation:

$$\bar{\sigma}_l = E\varepsilon \quad (0 \le |\varepsilon| \le |\varepsilon_t| \le 0.2) \tag{7}$$

$$\sigma_e = a\, e^{b\varepsilon} \Rightarrow \bar{\sigma}_e = a(1+\varepsilon)e^{b\varepsilon} \quad (|\varepsilon_t| \le |\varepsilon| \le |\varepsilon_y|) \tag{8}$$

Requirements for continuity between the linear and exponential regions:

$$\bar{\sigma}_l(\varepsilon_t) = \bar{\sigma}_e(\varepsilon_t) \tag{9}$$

$$\bar{\sigma'}_l(\varepsilon_t) = \bar{\sigma'}_e(\varepsilon_t) \tag{10}$$

where ε is the compression strain ($\varepsilon<0$) or tension strain ($\varepsilon>0$). The transition strain, ε_t is the strain at transition from the initial linear region to the exponential region and ε_y is the limit of validity of the exponential stress–strain relationship. Solving the set of Eqs. (7)–(10), yields the combined expression, covering both the linear and the exponential region ($0 \le |\varepsilon| \le |\varepsilon_y|$) as:

$$\bar{\sigma} = \frac{1+\varepsilon}{1+\varepsilon_c} E\varepsilon_c \exp\left\{\frac{\varepsilon-\varepsilon_c}{\varepsilon_c(1+\varepsilon_c)}\right\},$$

$$\sigma = \frac{E\varepsilon_c}{1+\varepsilon_c}\exp\left\{\frac{\varepsilon-\varepsilon_c}{\varepsilon_c(1+\varepsilon_c)}\right\} \tag{11}$$

$$\varepsilon_c = \varepsilon \quad (0 \le |\varepsilon| \le |\varepsilon_t|) \qquad \varepsilon_c = \varepsilon_t \quad (\varepsilon_t \le |\varepsilon| \le |\varepsilon_y|)$$

From a plot of σ versus ε, the two parameters E and ε_t may be found by regression of both regions combined ($0 \le |\varepsilon| \le |\varepsilon_y|$). A quicker method is to perform a linear regression of the logarithmic expression of the exponential region:

$$\ln|\sigma_e| = b\varepsilon + \ln|a| \tag{12}$$

To be able to relate the failure stress (σ_b) to the failure strain (ε_b) a factor, describing the deviation between the measured σ_b and the value calculated from ε_b by extrapolation from the exponential region, is introduced. This factor, $\sigma_{b,m/e}$, is defined as σ_b(measured)/σ_b(extrapolated) and yields $\sigma_{b,m/e}=1$ if failure occurs within the exponential region. The relation between stress and strain at failure is thus described by:

$$\sigma_b = \sigma_{b,m/e}\frac{E\varepsilon_t}{1+\varepsilon_t}\exp\left\{\frac{\varepsilon_b-\varepsilon_t}{\varepsilon_t(1+\varepsilon_t)}\right\} \tag{13}$$

Substituting, $a'=a/E$, in Eq. (12) yields:

$$\ln|\sigma_b| = b\varepsilon_b + \ln E + \ln|a'| + \ln \sigma_{b,m/e} \tag{14}$$

which is suitable for a phenomenological comparison of Figs. 5–9. Eq. (11) is empirically based on an observed behaviour during uniaxial compression = biaxial tension. The meaning of the transition strain (ε_t) is thus limited to the strain value for which the gels stress response to strain changes from that described by ideal rubber elasticity to an exponential nominal stress dependency.

Eq. (11) in terms of the extension ratio λ yields for simple compression ($1 \ge \lambda \ge \lambda_y$) or tension ($1 \le \lambda \le \lambda_y$):

$$\bar{\sigma} = E\lambda\frac{\lambda_c-1}{\lambda_c}\exp\left\{\left(\frac{\lambda-1}{\lambda_c-1}-1\right)\frac{1}{\lambda_c}\right\} \tag{15}$$

where λ_c, λ_t and λ_y are related to ε_c, ε_t and ε_y, respectively. For the exponential region the expression is observed to be analogues to the expression of Fung in simple tension (Eq. (4)), the parameters $1/c$ and α expressed as follows:

$$\frac{1}{c} = E\frac{\lambda_t-1}{\lambda_t}\exp\left\{\frac{1}{1-\lambda_t}\right\}, \alpha = \frac{1}{\lambda_t(\lambda_t-1)} \tag{16}$$

The strain energy per unit volume for the exponential region is thus given by the same equation as Fung's equation for tensile strain (Eq. (6)). In relation to measurements on soft tissue it may be noted that the determination of ε_t and λ_t from the exponential region of the stress–strain relationship does not depend on absolute strain, but may be derived from

relative strain without the knowledge of the absolute unstrained state.

3. Results and discussion

3.1. Gel geometry and appearance

For each gel, the diameter (d) and the height (l) was measured and the swelling ratio (V/V_0) calculated. The time dependent change of gel volume upon storing varied from a small degree of shrinkage to a considerable degree of swelling depending on the incubation solution and the duration of incubation. The values of d and l were also used for the evaluation of the gels ability to support their own weight during rheological investigation. Fig. 2 shows the relation between l/l_0 and d/d_0 for several gels studied here. The freshly molded gel is used as the Reference State and is thus characterized by $l/l_0 = 1$ and $d/d_0 = 1$. The diagonal line depicts a constant relation between l/l_0 and d/d_0, i.e. $(l/l_0)/(d/d_0) = 1 = (l/d)/(l_0/d_0)$, characteristic of an isotropic volume change (Fig. 2). Most of the gels are observed along this line, and therefore, displayed isotropic swelling or shrinkage relative to Reference State. Deviations in most cases resulted from gels not supporting their own weight when removed from solution. The gels that displayed true anisotropic swelling behavior were those stored in MQ-water or in solution of pH 13 (Table 2).

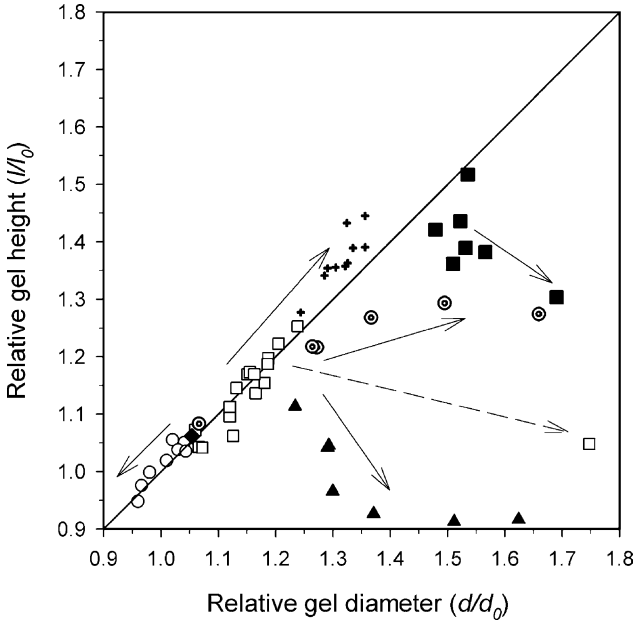

Fig. 2. Sample curves illustrating the different observed behaviours in the relationship between gel height l and gel diameter d upon storage. The main time-dependent changes illustrated by arrows. Common initial state before incubation (♦), SclGel$_{T21,\ 0.1\ M\ CaCl_2}$ (○), SclGel$_{T21,\ H_2O}$ (✚), SclGel$_{T96,\ H_2O}$ (■), SclGel$_{T96,\ 0.1\ M\ NaCl}$ (□), SclGel$_{T96,\ 1\ M\ CaCl_2}$ (◎) and SclGel$_{T21,\ pH\ 13}$ (▲).

All gels were initially washed in 0.1 M NaCl. This procedure was accompanied by an isotropic swelling to $l/l_0 = d/d_0 \approx 1.06$ (Fig. 2). Following this, differences were observed depending on the incubation conditions and duration. In Table 2, the studied systems are grouped according to the swelling behaviour focusing on changes in geometry.

Fig. 3(a) shows an image of a freshly moulded, slightly turbid gel. The gel is cylindrical with a tiny brim at each end surface. The gel illustrated in Fig. 3(b) was stored in 1 M NaCl at 96 °C for 29 days. Submerged in solution this gel was also cylindrical. The image also illustrates the change from the original turbid gel in Fig. 3(a) to a more transparent one; a feature observed for some incubation conditions (Table 2).

3.2. Large deformation measurements

Most gels adhered to the surfaces of the test geometry making it possible to perform limited elongation without any further attachment. The stress–strain measurement is illustrated in Fig. 3(c). By convention, compression results in negative strain and stress. For simplicity, the compression strain and stress is presented as positive values in Figs. 3–9. (i) Compression to $|\varepsilon| = 0.2$. (ii) Return to $\varepsilon = 0$. (iii) Further elongation of the distance between the upper and the lower test geometry, here presented as negative strain, correspond to stretching the gels. In particular, the heat-treated gels and the gels stored at pH 13 displayed good adhesion to the surfaces of the test geometry on elongation. (iv) The return of the measured stress to zero or to a constant, negative value, correspond to the gel detaching from the upper part or the lower part of the test geometry. For comparison, the stress–strain data for a gel stored in 0.1 M $CaCl_2$ at 21 °C for 694 days is shown (Fig. 3(d)). This gel displays the more typical response, though with a rather high value for Young's modulus (10.8 kPa). In some experiments, the gels were continuously cycled between compression and extension. For self-supporting gels, the measurements followed the same hysteresis loop, partly illustrated by arrows (i)–(iii) in Fig. 3(c), on subsequent deformation cycles. The variation in the gel height, determined by a deformation force of 0.01 N, between two subsequent runs on the same gel was in general within $\pm 0.1\%$. For gels incubated in MQ-water a reduction of the height in the order of 1% and for gels incubated at 96 °C in the order of 3–4% was observed on the second deformation cycle of a gel.

The following trends, listed in order of appearance, were observed for most degrading gels; decreasing ε_b and σ_b, decreasing E, increasing V/V_0 and decreasing pH of the incubation solution, loss of ability to support its own weight when removed from solution and finally dissolution of the gel. No fragmentation was observed during degradation. On prolonged storage of the dissolved gels, incubated at 96 °C, a change of colour to a yellowish brown and a development of a characteristic smell of caramel, were observed in

Table 2
Overview of appearance and swelling behaviour of scleroglucan renaturation gels incubated under various conditions

Incubation conditions	Swelling behaviour	Optical appearance
NaCl and $CaCl_2$, pH 1, 2 and 12 at 21 °C	Isotropic swelling; similar in appearance to the freshly moulded gel in Fig. 3(a)	$I=3$ M, transparent, slightly yellow; $I=0.1$ and 1 M, slightly turbid pH 12; transparent pH 1 and 2; turbid
H_2O at 6 and 21 °C	Anisotropic swelling ($l/l_0 > d/d_0$) due to a curvature of the end surfaces of the gel cylinders	Slightly turbid
H_2O, NaCl and $CaCl_2$ at 96 °C	Initially, isotropic swelling followed by apparent anisotropy[a] (image in Fig. 3(b))	Transparent. Slightly yellowish brown at high ionic strength
pH 13 at 21 °C	Quickly became weak, changing appearance from well-defined cylinders to less defined spheres with a sticky surface	Transparent

[a] The apparent anisotropy ($l/l_0 < d/d_0$) was observed for gels not supporting their own weight.

approximately half of the bottles, indicative of caramelisation.

Gels incubated in solution of pH 13 displayed the common features of degrading gels, but additionally a change in geometry from the original cylindrical towards a more spherical one, even in solution, was observed. The surface of the gels also seemed to become less defined and stickier. The overall rate of change in gel properties was faster than for other conditions, including incubation at 96 °C.

Important parameters governing the observed geometrical and low deformation mechanical properties of the incubated gels are the number of elastically active segments per unit volume (υ'), the nature of each of these segments and the parameters determining the swelling equilibrium of the gel. For gels displaying both

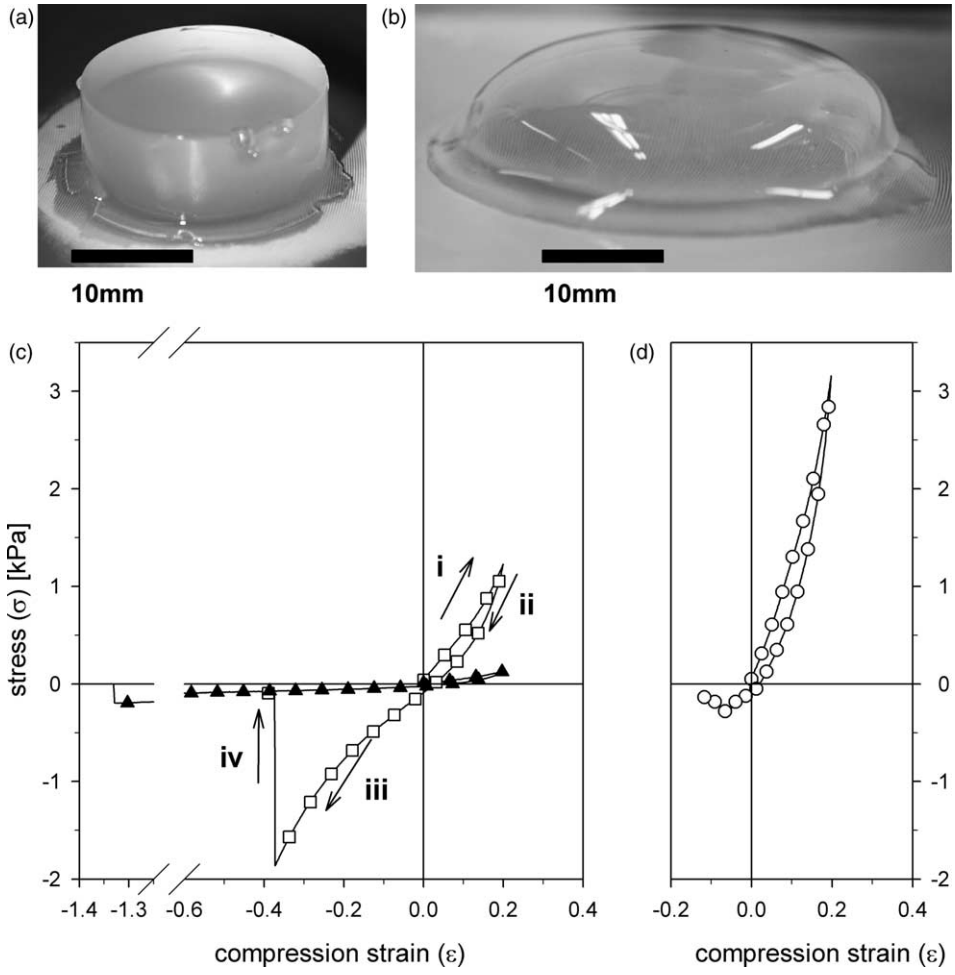

Fig. 3. (a) A freshly molded gel. (b) A gel stored in 1 M NaCl at 96 °C for 29 days. (c) Compression/elongation runs for $SclGel_{T21,\ pH\ 13,\ t=0.28\ days}$ (▲) and $SclGel_{T96,\ 0.1\ M\ NaCl,\ t=0.95\ days}$ (□). (d) Compression/elongation run for $SclGel_{T21,\ 0.1\ M\ CaCl_2,\ t=694\ days}$ (○). The data acquisition rate was 12.5 s^{-1} at 0.1 mm s^{-1}, symbols presented for 1 of 60 data points. The gels in (a) and (b) do not correspond to any of the illustrated curves in (c) and (d).

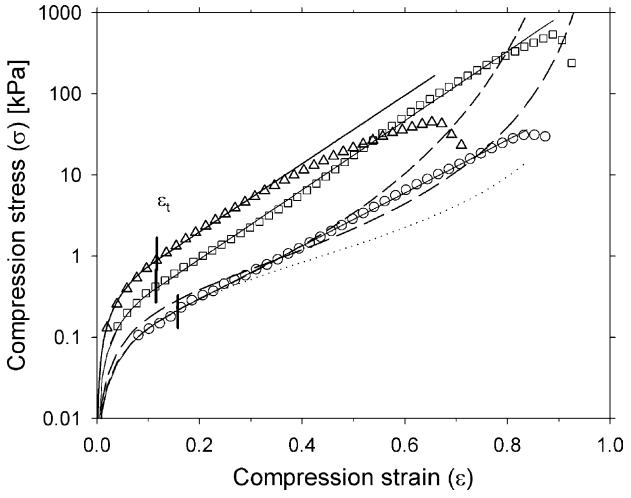

Fig. 4. Fitting of experimental data to a combined linear and exponential expression (Eq. (11)) for $SclGel_{T6,\ 0.1\ M\ NaCl,\ t=697\ days}$ [$\varepsilon_t=-0.117$, $E=6.7$ kPa] (△), $SclGel_{T96,\ 0.1\ M\ NaCl,\ t=0.15\ h}$ [$\varepsilon_t=-0.158$, $E=1.15$ kPa] (○) and $SclGel_{T96,\ 0.1\ M\ NaCl,\ t=5.9\ h}$ [$\varepsilon_t=-0.115$, $E=3.1$ kPa] (□). Vertical lines are given for the regression parameter, $\varepsilon=\varepsilon_t$, the transition between the linear and exponential region of a fit. Extrapolation of the linear region (···). Fit to the BST equation (- - -), upper [$n=8.0$, $E=1.26$ kPa], lower [$n=4.3$, $E=1.61$ kPa].

changes in the equilibrium volume and in Young's modulus, the ratio:

$$R_x = \frac{E}{E_0}\left(\frac{V_0}{V}\right)^{1/3} \tag{17}$$

was calculated. This reflect the ratio between the number of elastically active network chains in the swollen state following incubation relative to the reference state (Treloar, 1975). In the low deformation region of the Gaussian network theory, observed deviations from $R_x=1$ indicate changes in crosslink densities having occurred during the storage.

The strain at failure, ε_b, for homogeneous networks of comparable structures, is likely to depend more on the nature of the individual chains, than on the number of them. The stress at failure, σ_b, in turn, is determined both by the number of active chains (through E) and the nature of them (through ε_b and $\sigma_{b,m/e}$) (Eqs. (11)–(14)). Fig. 4 shows three examples of experimental data fitted by least squares of the residuals of the logarithms to Eq. (11). In performing such a fit it is of importance to know the exact unstrained state. The measured curves of force versus compression deformation were extrapolated by regression from the trigger point ($F=0.01$ N) back to the actual unstrained state. The gel stored at 6 °C (upper curve) best illustrates a scleroglucan renaturation gel. For this gel it was difficult to determine the value of ε_y, in fact it was difficult to determine whether there is a real exponential region. Regression from $\varepsilon=0$ to $0.5\varepsilon_b$ ($\varepsilon_b=-0.66$) yielded $E=6.7$ kPa, in good agreement with $E_{init}=6.4$ kPa as determined from the initial linear region. The transition strain was determined to $\varepsilon_t=-0.12$ and $\sigma_{b,m/e}=0.27$. Extending the regression region illustrated the deviation from an exponential stress–strain relation, both E and ε_t was forced upwards. A regression of the curve from $\varepsilon=0$ to ε_b yielded $E=7.6$ kPa and $\varepsilon_t=-0.15$. The gel annealed for 0.15 h at 96 °C shows a more distinct exponential region. Whether regression was performed from $\varepsilon=0$ to $0.5\varepsilon_b$ or from $\varepsilon=0$ to ε_b ($\varepsilon_b=-0.84$), the same parameter values were obtained ($E=1.15$ kPa and $\varepsilon_t=-0.16$) while $E_{init}=1.10$ kPa. For the regression from $\varepsilon=0$ to $0.5\varepsilon_b$, $\sigma_{b,m/e}=0.88$ was determined. Extrapolation of the initial linear region to values above $|\varepsilon_t|$ is illustrated by the dotted line. As the BST-equation (Eq. (2)) yields stronger upward curvature at high strain than the exponential expression (Eq. (11)) the two will differ at sufficiently high strain. The two dashed lines illustrate fits of the experimental data to the BST-equation. The fit of the data from $\varepsilon=0$ to $0.5\varepsilon_b$ ($n=8.0$, $E=1.26$ kPa) is seen to correspond well with the experimental data within this region. The extrapolation, however, does not hold at all. Fitting the whole curve (from $\varepsilon=0$ to ε_b) yielded $n=4.3$ and $E=1.61$ kPa. A better fit of the high strain region was gained at the expense of the fit in the low strain region. The BST-equation was also less suitable than the exponential equation for fitting the first mentioned data as this curve shows a downward curvature at high strain, as plotted in Fig. 4. The last set of data in Fig. 4, also yielded good fit to Eq. (11). These data are for a gel annealed for 5.9 h at 96 °C. Fitting from $\varepsilon=0$ to $0.7\varepsilon_b$ ($\varepsilon_b=-0.89$) yielded $E=3.2$ kPa, $\varepsilon_t=-0.12$ and $\sigma_{b,m/e}=0.67$. Compared with the gel annealed for 0.15 h in relation to Eqs. (11)–(14), the increase in E from 1.15 to 3.2 kPa is seen to have shifted the initial linear region upward. The decrease in $|\varepsilon_t|$ from 0.16 to 0.12 implies a transition to an exponential stress–strain relation at a lower degree of deformation. Implicit, it also yields a higher exponential exponent, both increasing σ_b. The effect on σ_b from the increase in $|\varepsilon_b|$ from 0.84 to 0.89 is much larger than the effect of the reduction in $\sigma_{b,m/e}$ from 0.88 to 0.67.

When a clearly identifiable exponential region existed, values of ε_t and E found by Eq. (12) differed less than 5% from values found by the more elaborate method above.

The influence on the predicted σ_b by Eq. (13), from changes in the equation parameters, one at the time, is illustrated in Table 3. The chosen values does not present limiting values for the parameters, but are variations within a reasonable range as observed for the data in Figs. 5–9. For a representative set of initial values, each of the parameters E, ε_t, ε_b, $\sigma_{b,m/e}$ are varied within reasonable limits. The failure strain is seen as the single most important parameter, followed by the Young's modulus. A qualitative comparison of the experimental values of σ_b, E and ε_b (Figs. 5, 6, 8 and 9) according to Eq. (14) seems justified without detailed characterisation of the two other parameters. From our experimental data $\ln(\sigma_b)$ is in general observed to relate to the changes in $\ln(E)$ and ε_b as expected from Eq. (14).

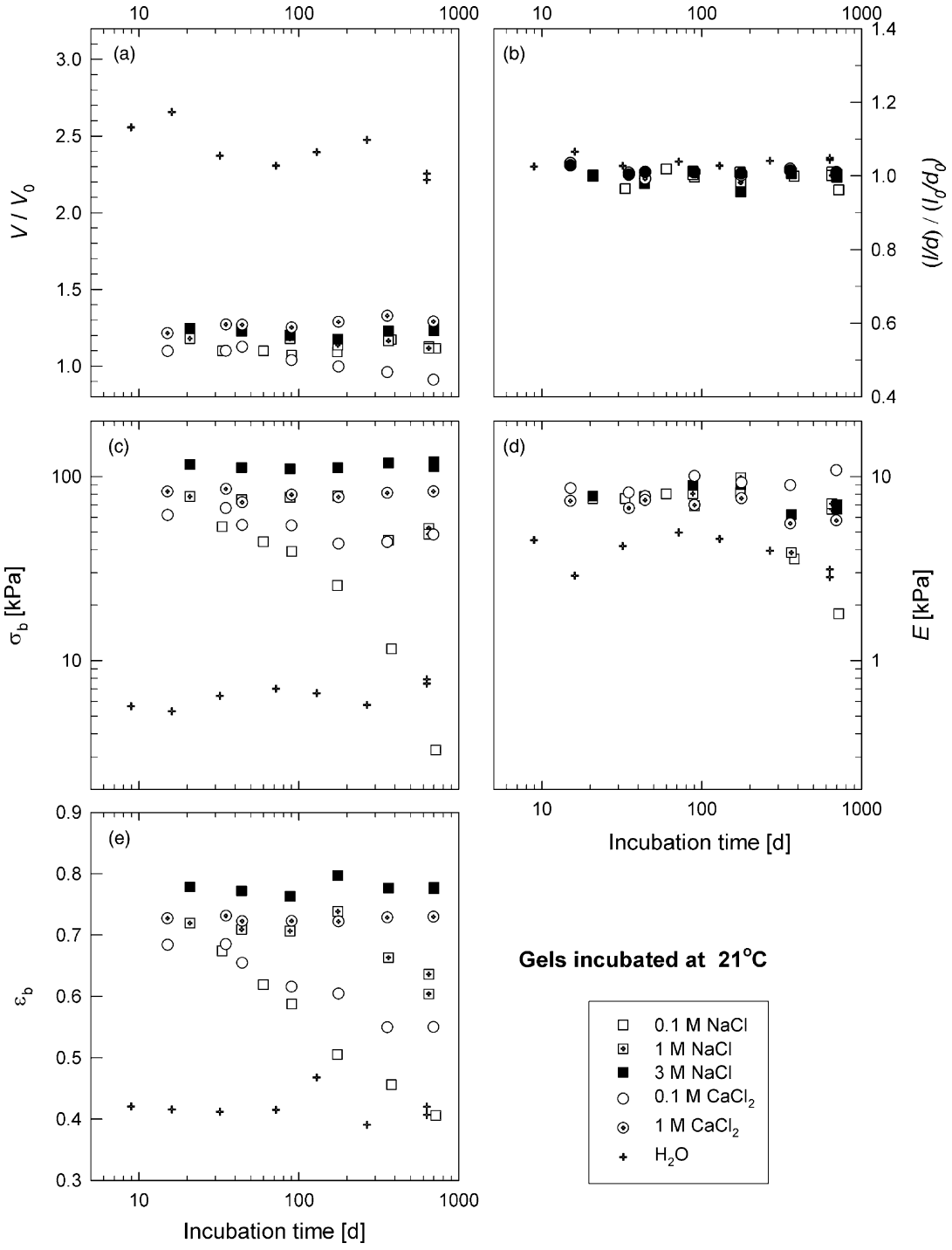

Fig. 5. Dependence of the incubation time for gel properties of gels moulded from a 5% scleroglucan solution and incubated at 21 °C. (a) Relative volume, (b) change in the height/diameter ratio (l/d), (c) stress at gel failure (σ_b), (d) Young's modulus, (e) strain at gel failure (ε_b). Incubation conditions; SclGel$_{T21,\ H_2O}$ (✚), SclGel$_{T21,\ 0.1\ M\ NaCl}$ (□), SclGel$_{T21,\ 1\ M\ NaCl}$ (⊡), SclGel$_{T21,\ 3\ M\ NaCl}$ (■), SclGel$_{T21,\ 0.1\ M\ CaCl_2}$ (○), SclGel$_{T21,\ 1\ M\ CaCl_2}$ (◎).

One should note here, that the measurements were performed at a finite compression rate, and therefore, do not necessarily reflect a relaxed network. Both the course and the final values depend on the kinetics of the measurements. The applied compression speed, $\Delta l/\Delta t = 0.1\ \mathrm{mm\ s^{-1}}$ was the lowest available for our measurements. Compressing the gels at this speed to a given strain, then relaxing the network for 100 s before measuring gave curves of similar shape as presented in Fig. 4. This was also the case for increased $\Delta l/\Delta t$ up to the highest tested value of $5\ \mathrm{mm\ s^{-1}}$. A detailed investigation was not performed on the effect of the deformation speed. The general observed trends with increasing $\Delta l/\Delta t$ was increasing E and increasing σ_b. The effect on ε_b was not

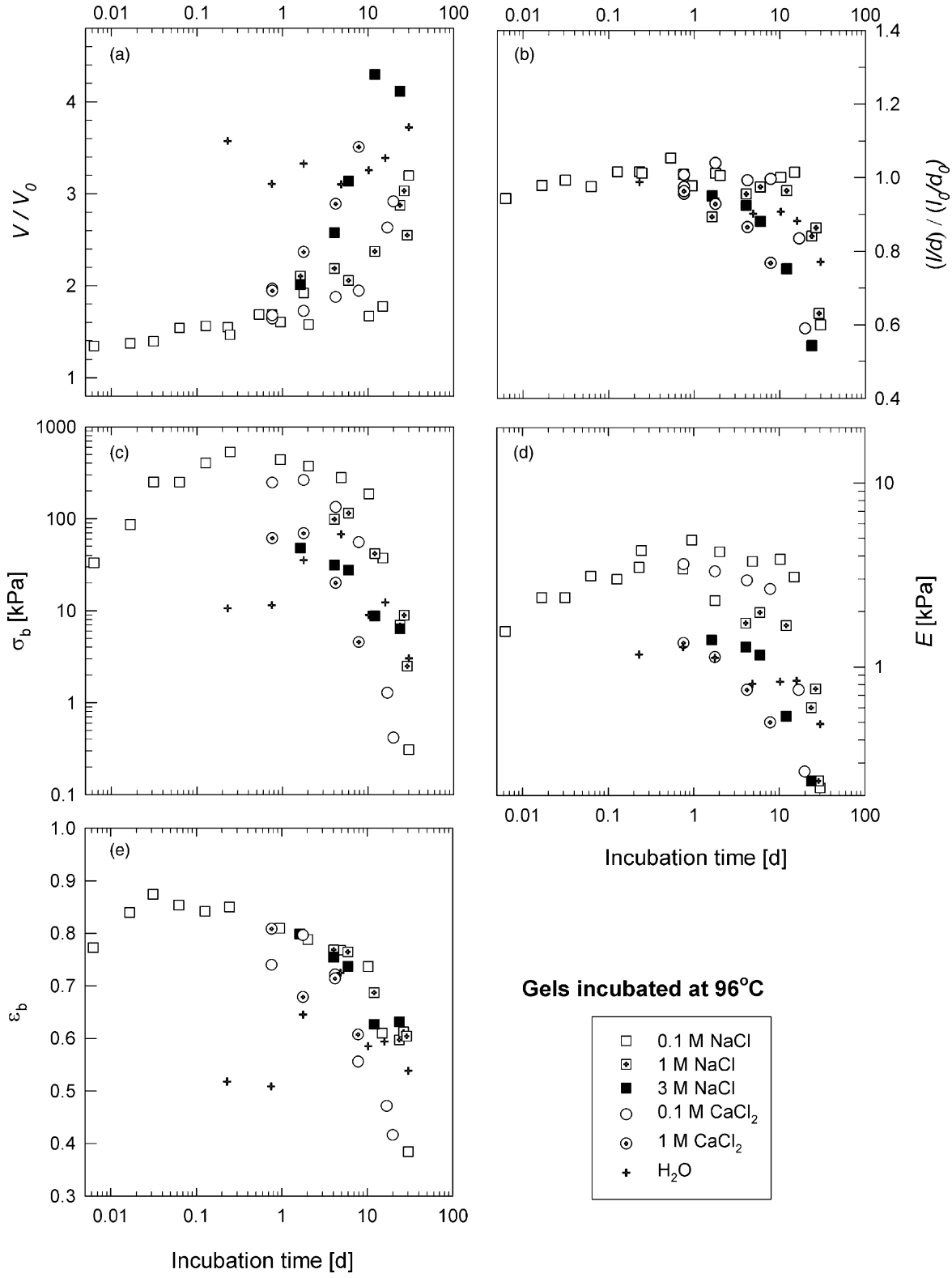

Fig. 6. Dependence of the incubation time for gel properties of gels moulded from a 5% scleroglucan solution and incubated at 96 °C. (a) Relative volume, (b) change in the height/diameter ratio (*l*/*d*), (c) stress at gel failure (σ_b), (d) Young's modulus, and (e) strain at gel failure (ε_b). Incubation conditions; $SclGel_{T96,\ H_2O}$ (✚), $SclGel_{T96,\ 0.1\ M\ NaCl}$ (□), $SclGel_{T96,\ 1\ M\ NaCl}$ (⊡), $SclGel_{T96,\ 3\ M\ NaCl}$ (■) and $SclGel_{T96,\ 0.1\ M\ CaCl_2}$ (○), $SclGel_{T96,\ 1\ M\ CaCl_2}$ (◎).

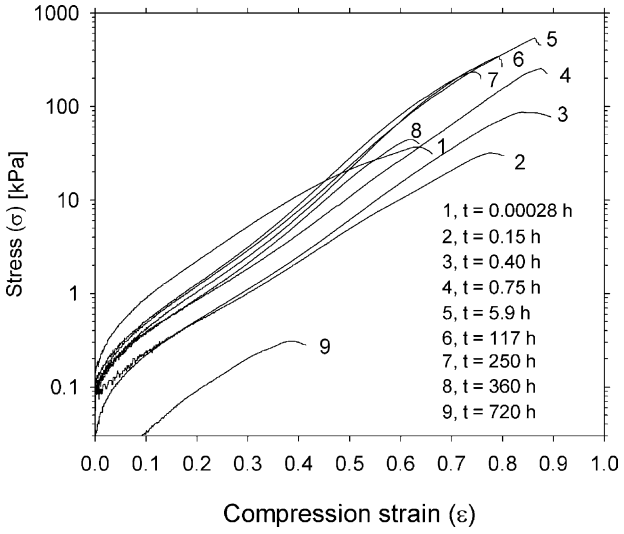

Fig. 7. Stress–strain measurements of gels stored in 0.1 M NaCl at 96 °C.

so obvious from the limited testing. Gel failure could, however, be induced by holding the gel at a deformation close to, but below the reported ε_b values for $\Delta l/\Delta t = 0.1\ \mathrm{mm\ s^{-1}}$. This indicates an increase in ε_b with increasing deformation speed at low and moderate values of the latter. This observed time dependent fatigue of the network under compression also contributes to the broadening of the gel failure curve. A gel displaying a broader failure profile would more likely resemble a thick solution after gel failure. The gels displaying sharp failure curves as illustrated by the annealing gels in Fig. 4, would in general be more resilient and show less pronounced fatigue failure on repeated deformation cycles. These gels also displayed the most marked exponential region of stress–strain.

The scleroglucan gel network can be viewed to consist of rigid rods made up of triple helical junction zones interconnected through single stranded segments. The initial deformation ($|\varepsilon| < |\varepsilon_t|$) is expected to be associated with a Gaussian statistical response while the rod-like junction zones are displaced but not deformed. Deformation of the junction zones occur with increasing influence the larger the deformation. The transition strain, ε_t, does not necessarily imply a limit of Gaussian extensibility of elastically active chains and onset of deformation of the rod-like segments. An exponential stress–strain relation may be modelled from

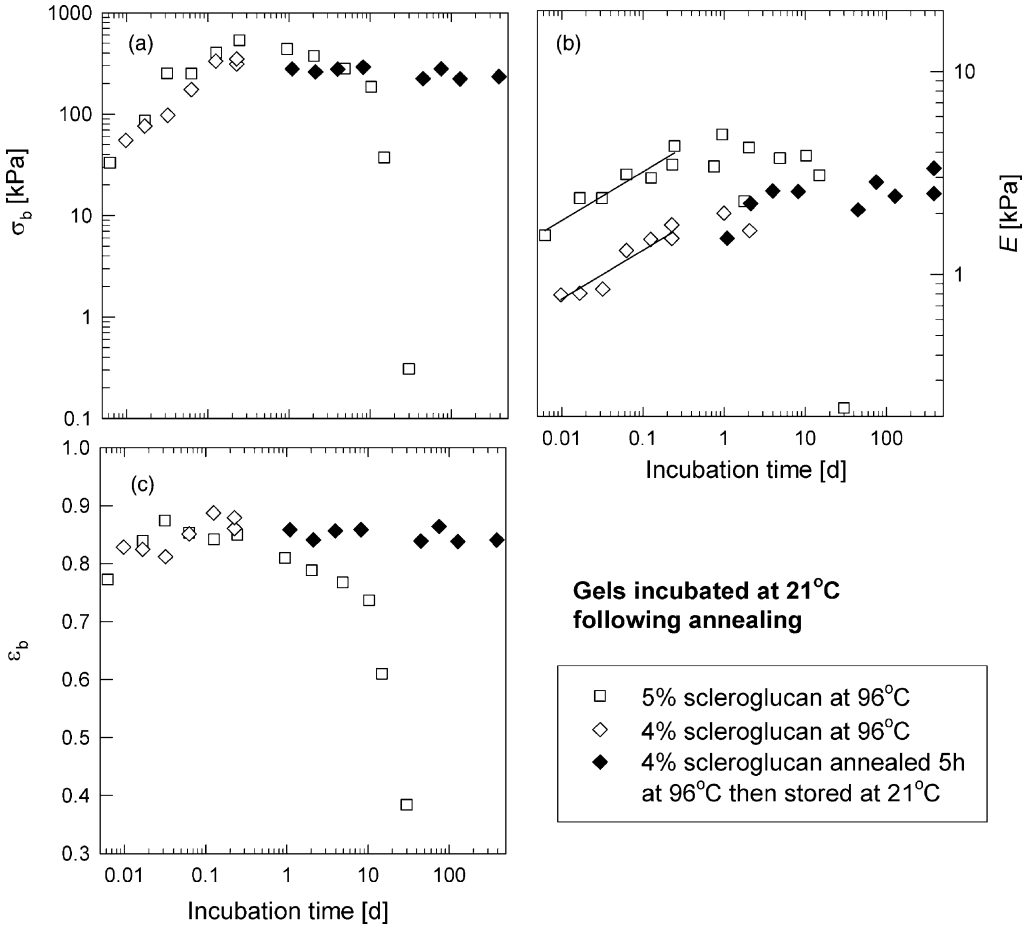

Fig. 8. Dependence of the incubation time for gel properties of gels moulded from a 5% scleroglucan solution and incubated at 21 °C following annealing. (a) Relative volume, (b) change in the height/diameter ratio (l/d), (c) stress at gel failure (σ_b), (d) Young's modulus, and (e) strain at gel failure (ε_b). Gels (5%) incubated at 96 °C, $\mathrm{SclGel_{T96,\ 0.1\ M\ NaCl}}$ (□), gels (4%) incubated at 96 °C (◇), and the latter incubated at 21 °C after 5 h incubation at 96 °C, $\mathrm{SclGel_{T96>21,\ 0.1\ M\ NaCl,\ 4\%}}$ (◆).

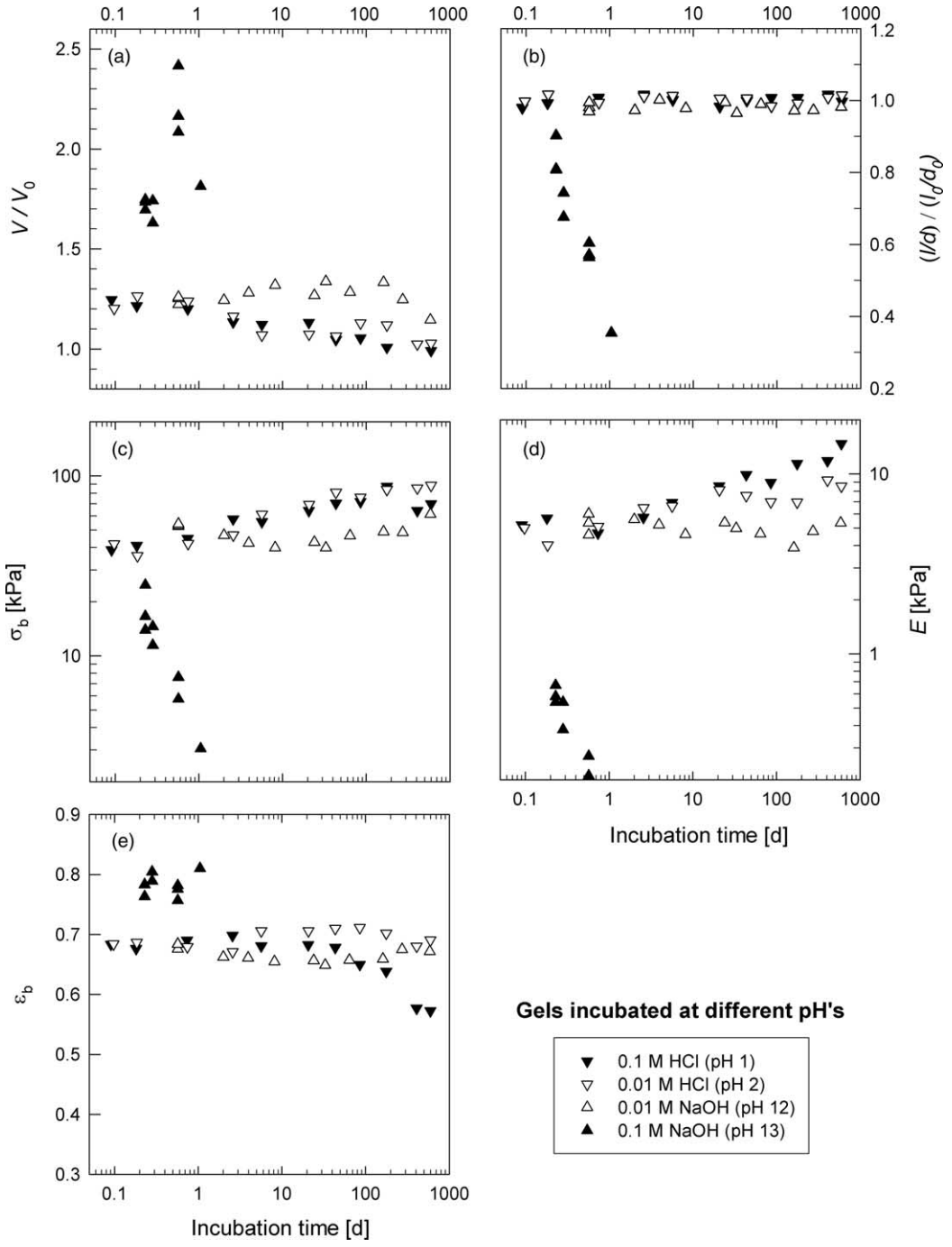

Fig. 9. Dependence of the incubation time for gel properties of gels moulded from a 5% scleroglucan solution and incubated at different pH's. (a) Stress at gel failure (σ_b), (b) Young's modulus, and (c) strain at gel failure (ε_b). Incubation conditions; $SclGel_{T21,\ pH\ 1}$ (▼), $SclGel_{T21,\ pH\ 2}$ (▽), $SclGel_{T21,\ pH\ 12}$ (△), $SclGel_{T21,\ pH\ 13}$ (▲).

the interconnection of Hookean springs (Becker et al., 2003). Another possible reason for the transition is that other deformation mechanisms, i.e. in the direction of compression might become dominating above $|\varepsilon_t|$. Fitting the limited uniaxial tension measurement curves to Eq. (11) yielded comparable values of E as obtained from the compression curves, but markedly higher transitional strain $|\varepsilon_t|$. For instance the extension region of the illustration gel, marked (iii), in Fig. 3(c) yielded $E = 4.1$–4.6, while the extended compression measurement (not shown) yielded $E = 4.8$. The extension ratio of transition in uniaxial tension ($\lambda_{t,UT}$) equaled 1.17 while the equivalent in biaxial tension ($\lambda_{t,BT}$) as obtained from the uniaxial compression measurement was 1.05. The corresponding extension ratios in compression were observed to be closer related, $\lambda_{t,UC} = 0.91$ and $\lambda_{t,BC} = 0.93$.

Table 3
The dependence of the predicted σ_b by Eq. (13) on the parameters of the equation, one changed at the time

Observed parameter	Set 1		Set 2		σ_{b2}/σ_{b1}
	Parameter value 1	Predicted $\lvert\sigma_{b1}\rvert$ (kPa)	Parameter value 2	Predicted $\lvert\sigma_{b2}\rvert$ (kPa)	
E (kPa)	1	10	10	99	10
ε_t	−0.16	22	−0.11	108	5
ε_b	−0.4	4	−0.9	462	116
$\sigma_{b,m/e}$	0.2	46	0.9	209	5

Initial chosen values; $E=7$ kPa, $\varepsilon_t=-0.12$, $\varepsilon_b=-0.7$, $\sigma_{b,m/e}=0.3$; yielding $\sigma_b=-70$ kPa.

3.3. Incubation at 6 and 21 °C

Fig. 5 shows the properties of gels moulded from 5% scleroglucan solutions, incubated at 21 °C. The properties of similar gels stored at 6 °C shows similar trends as those observed at 21 °C, except that the gels stored in 0.1 M NaCl also were stable at 6 °C (data not shown). Incubation at 6 °C with added formaldehyde to the incubating solutions also showed that formaldehyde did not directly influence the properties of the incubated gels. For gels stored in the solutions of 0.1 M NaCl and $CaCl_2$, a weakened gel network was observed after more than 30 days of incubation at 21 °C while this was not the case for the gels stored at 6 °C. Visual impurities typical of contamination were observed in the incubation solutions of these gels.

The initial steps were common for all gels, i.e. moulding and washing in 0.1 M NaCl at 6 °C. The properties of these gels, depending little on incubation time, represent the common initial Reference State for all gels. The major changes in mechanical and geometrical properties relative to the 0.1 M NaCl, 6 °C-incubated gels were observed pre-incubation, during washing in the respective incubation solutions. During the following more than 600 days of incubation, only minor time-dependent changes were in general observed for the mechanical and geometrical properties. All the gels displayed isotropic swelling behaviour.

A constant swelling ratio (V/V_0) of 2.2–2.5 was observed for the gels incubated in MQ-water independent on the duration of the storage (Fig. 5(a)). The gel volume was observed to depend slightly on the ionic strength of the incubation solution for $I\geq 0.1$ M with V/V_0 increasing with increasing I. Gels incubated in 0.1 M $CaCl_2$, were exceptions, yielding initially lower swelling ratios, $V/V_0\in$ 1.05–1.12, than expected based only on the ionic strength ($I=0.3$ M). A further time dependent decrease in the swelling ratio was observed for gels incubated in 0.1 M $CaCl_2$ at 21 °C, yielding $V/V_0=0.91$ after 694 days of incubation.

Incubation in MQ-water yielded the lowest values of Young's modulus ($E\in$3–5 kPa) (Fig. 5(d)) and strain at failure ($\lvert\varepsilon_b\rvert\in$0.4–0.5). In accordance with Eq. (13) the same is observed for the stress at failure ($\lvert\sigma_b\rvert\in$6–9 kPa) (Fig. 5(c)). The gels incubated in solutions of $I\geq 0.1$ M displayed only minor differences in the Young's modulus ($E\in$7–10 kPa) and thus σ_b is seen to relate well to ε_b. Increasing values of $\lvert\varepsilon_b\rvert$ and $\lvert\sigma_b\rvert$ were observed with increasing ionic strength within the range $\lvert\sigma_b\rvert\in$40–120 kPa and $\lvert\varepsilon_b\rvert\in$0.64–0.78 at 21 °C (Fig. 5). For gels incubated at 6 °C similar initial values were observed. It is rather unlikely that a major rearrangement of the gel network would take place at ambient temperatures at $I\geq 0.1$ M. The similar swelling ratios and Young's modulus, yielded estimates of $R_x\in$0.9–1.1 throughout the 719 days of storage, for gels incubated at these conditions supporting this theory. Still, the increase in $\lvert\varepsilon_b\rvert$ and $\lvert\sigma_b\rvert$ with increasing I suggests a stabilisation of the gel network increasing the ability to withstand deformation.

A time dependent microbial degradation was observed for gels incubated in 0.1 M NaCl or 0.1 M $CaCl_2$ at 21 °C. A marked and continuous decline in $\lvert\sigma_b\rvert$ and $\lvert\varepsilon_b\rvert$ was observed for $t\geq 30$ days, $\lvert\sigma_b\rvert$ decreasing more than a decade within 719 days for the former. Decreasing values of $\lvert\varepsilon_b\rvert$ for gels incubated in 1 M NaCl at 21 °C for $t\geq 363$ days may indicate a beginning degradation. The decrease in E for gels incubated in 0.1 M NaCl was not accompanied by a change in the V/V_0 and was, therefore, proportional to the decrease in the number of elastically active chains, the R_x parameter was calculated to 0.25 at $t=719$ days.

3.4. Swelling

Guo, Elgsaeter, Christensen, and Stokke (1998) investigated the effect of the charge density on swelling of sclerox-chitosan gels in ionic aqueous solution. Among the studied systems were polyanionic gels, i.e. were the cationic contribution from the chitosan could be disregarded. Data for V/V_0 versus salt concentration were fitted to the theory of swelling of polyelectrolyte gels, in short:

$$\Pi_{elas}+\Pi_{ion}+\Pi_{mix}=0 \tag{18}$$

where Π_{elas}, Π_{ion} Π_{mix} are the contribution to the osmotic swelling pressure of the gel from elastic deformation, Donnan equilibrium, and mixing of the polymer chains with solvent, respectively. Gels made from 1.04% solutions of sclerox with varying degree of carboxylation (0, 0.05, 0.12 and 0.18) were fitted varying the parameters $\upsilon'=\upsilon/V_0$ (the number of elastic active polymer chains per volume), χ (the Flory–Huggins parameter), λ_{max} (the maximum extension ratio of the polymer chain) and M_2 (the molar mass of polymer per unit charge). In the present study the lack of

detailed swelling data within $I \in 10^{-7}$–10^{-1} M, does not permit a detailed numerical fitting to the theory, but some trends can be deduced. A plateau-value is expected for V/V_0 at low ionic strength, here represented by the gels incubated in MQ-water. Similarly, the plateau of V/V_0 previously observed for high ionic strengths can be expected to contain the present data for [NaCl] ≥ 0.1 M. Using this theory, the differences in V/V_0 of these two plateaus could be accounted for using parameter values in accordance with the previous data and observations of mechanical properties reported here. In specific, using $\chi = 0.46$, $\lambda_{max} = 3$, $\upsilon' \in (1\text{–}1.5)\ 10^{23}\ m^{-3}$, $M_2 = 37{,}500$ g/mol (consistent with $D_c = 0.017$) for the 5% gels, the theory predicts $V/V_0 \approx 1.2$ and 2.3 for the high and low ionic strength plateaus, respectively. This finding suggest that the network charge density identified yields a sufficient driving force to account for the differences in equilibrium gel volume at low and high ionic strength.

3.5. Incubation at 96 °C—annealing and degradation

Fig. 6 shows the measured properties of gels moulded from a 5% scleroglucan solution then incubated at 96 °C. Stress–strain data obtained during the initial 3 days of incubation at 0.1 M NaCl provide more direct evidence of the change in the mechanical properties associated with the annealing process and the subsequent weakening of the gels (Fig. 7). Note that the data in Fig. 7 are not representative of the gels as they exist at 96 °C, but represent networks that can be kinetically trapped by cooling after incubation at different times at 96 °C. In Fig. 7, single runs, for each of the selected incubation times, are presented whereas Fig. 6 provides the average of several parallels. The stability of the annealed gels was studied by incubating gels at room temperature after 5 h of annealing (Fig. 8). The later was performed with gels moulded from a 4% solution of scleroglucan.

The gels initially displayed an approximate isotropic swelling behaviour (Fig. 6(b)) with linearly increasing volume with logarithmic time (0.006–15 days) (Fig. 6(a)). At the last observation ($t = 30$ days) a pronounced swelling had occurred and the gels were no longer self-supporting when removed from the incubation solution. Shortly after, all gels were degraded. The initial Young's modulus of the gels incubated in 0.1 M NaCl at 96 °C was 6–8 kPa (curve 1 in Fig. 7). In approximately 10 min, E dropped to a minimum of 1–1.5 kPa (Fig. 6(d); shift from curve 1 to curve 2 in Fig. 7). Apparently, a large fraction of the elastically active chains from the original renaturation network are no longer in effect. Simultaneously a marked increase in ε_b is observed. This increase continues for a little less than an hour under further incubation at 96 °C (curve 3 and 4, Fig. 7) while the number of elastically active chains is also increasing, as observed from Figs. 6(d) and 8(d) and by the upward shift of the curves in Fig. 7. The increase in E continues until the network simultaneously reaches a maximum in E and $|\sigma_b|$ after approximately 6 h. During this time period the gels turn transparent and the failure profile becomes markedly sharper as seen from curves 3–5 in Fig. 7. The most likely explanation for the observed changes is that a reorganisation of the gel network is taking place. The junction zones of the original rather heterogeneous renaturation network, is replaced by a more resilient network of more homogenous and presumably more perfectly aligned triple helixes. The highest transition strain is $|\varepsilon_t| = 0.16$ as observed for the gel annealed for 0.15 h (curve 2 of Fig. 7). A continuous decrease in $|\varepsilon_t|$ is observed until a minimum is reached at $|\varepsilon_t| = 0.11$ (curves 6 and 7). This decrease corresponds to a reduction in the Gaussian statistical region of compression and a correspondingly increase in non-linear behaviour as would be expected for the network dominated by rigid rods. The best simultaneous fit of the annealing for both the 4 and 5% gels (Fig. 8(d)) yields $E \propto t^{0.24}$. In the 'Rod and coils model' and its application to gelatine, Groot et al. (1996) interpret the increase of nonlinearity with time, as the growth of the rods. They find the rod length relative to the coil size to grow with $t^{0.26}$. They propose the growth of the rods may be diffusion controlled by the Rouse diffusion process (Rouse, 1953). This power law coefficient coincides with that observed here and may suggest that the observed increase in the elasticity is due to recruitment of elastically active network chains by a similar process.

When the gels were transferred to incubation at room temperature after annealing, they were observed to maintain the properties induced by the annealing procedure for the more than 400 days duration of incubation. For the 4% gels this was ($|\sigma_b| \in 220$–290 kPa, $E \in 2$–3 kPa and $|\varepsilon_b| \in 0.84$–0.86) (Fig. 8(c)–(e)). The gels were found to degrade when further incubated at 96 °C. Within the first 10 days, this was mainly observed as a reduction in ε_b indicating that the number of elastically active chains did not change a lot, but each chain anchoring became weaker. This could be the result of masked scissions in single strands of the triple helical junction zones. It could also result from a further alignment of triple helixes, reducing the elasticity of the gel network. The minimum in $|\varepsilon_t|$ is observed for these gels, showing a limited decrease in $|\varepsilon_b|$, not yet showing a decrease in E. When the final network degradation is observed it could be explained by the further development of either two of the possible routes above.

Incubation in 0.1 M NaCl at 96 °C reduced R_x (Eq. (17)) to 0.23 within 9 min. After 1 day, a maximum of 0.75 was reached following, which a steady decrease was observed to 0.49 after 15 days of storage. After 30 days, the value had dropped to 0.04.

The increase in σ_b during annealing was remarkable. Within 1 day, an increase from the initial value of 40 kPa to a value of more then 500 kPa was observed. According to Eq. (13), Fig. 4 and Table 3, the increase partly follows from the increase in E during the rebuilding of the annealed

network. The main contribution comes, however, from the high failure strain of the annealed network. An increase in $|\varepsilon_b|$ from the initial of 0.68 to more than 0.85 occurs within the first 45 min of annealing. Fig. 6(c) and (d) indicate that the gels stored in the solutions of 3 M NaCl and 1 M $CaCl_2$, do not reach the same high values of $|\sigma_b|$ and $|\varepsilon_b|$, as do the gels stored in 0.1 M NaCl (and perhaps 0.1 M $CaCl_2$). The stronger and more resilient renaturation networks (Fig. 5(c) and (d)) of the former might be of hindrance for the necessary rearrangement needed for the forming of strong gels following annealing. Although similar values are observed for ε_b, the number of elastically active chains and of E (Fig. 6(d)) is smaller.

The onset of the profound swelling and the distortion of the gel proportions occurred first for the gels stored in the solutions of the highest ionic strength (Fig. 6(a) and (b)). The gels stored in NaCl (1 and 3 M) and in $CaCl_2$ (1 M) were no longer self-supporting after 1.5 days of storage (Fig. 6(b)) and the exact values of these rheological data are thus uncertain. Although initially weaker, these gels were not observed to dissolve significantly earlier than the gels stored in 0.1 M NaCl (Fig. 6(c) and (e)). For gels stored in MQ-water an increased initial swelling ratio ($V/V_0 > 3$) was observed. During storage, a relatively constant volume was observed until the sudden dissolution occurred also for these gels after approximately 30 days of incubation.

3.6. Effect of pH

Fig. 9 shows the measured properties of gels, moulded from 5% scleroglucan solutions, incubated at room temperature at pH 1, 2, 12 and 13. No buffer was applied for pH control, but only minor variations in pH were observed during the 596 days of incubation.

The gels incubated in solutions of pH 13 behaved very different from other gels. After 0.3 day (7 h) a swelling ratio of $V/V_0 = 1.7$ was observed (Fig. 9(a)) and the gels no longer supported their own weight (Fig. 9(b)). After 1 day of storage, even careful handling damaged the gels.

The gels incubated at pH 1, 2 and 12 initially displayed very similar values for all geometrical and mechanical properties ($V/V_0 = 1.2$–1.3, $E = 5$ kPa and $|\varepsilon_b| = 0.68$, $|\sigma_b| = 40$ kPa) suggesting the ionic strength of the incubation solution ($I = 0.1$ M) being the determining factor. For $t <$ 200 days gels incubated at pH 12 displayed a limited time dependence compared to gels incubated at pH 1 or 2. The swelling ratio of gels incubated at pH 12 increased a little whereas a decrease was observed for gels stored at pH 1 and pH 2 upon storage (Fig. 9(a)). All gels displayed isotropic swelling behaviour (Fig. 9(b)). Gels stored at pH 1 and at pH 2 were observed to have the same overall time dependence. The Young's modulus was observed to increase most for the gels stored at pH 1, yielding values as high as 14.8 kPa after 598 days of incubation (Fig. 9(d)). The stress at failure increased linearly with logarithmic time for both conditions (Fig. 9(c)) yielding $|\sigma_b| = 85$ kPa (twice the initial) after 170 days of incubation. Only minor variations were observed for ε_b of gels incubated at pH 1, 2 and 12 for the first 170 days. Following this, a decline was observed for gels incubated at pH 1.

Parameter R_x was observed to increase from the initial value of 0.7 to a value of 2 after 598 days for the gels incubated at pH 1. The same trend was observed for gels incubated in pH 2, with R_x increasing from 0.7 to 1.2. Gels incubated at pH 12 yielded constant values $R_x \in 0.6$–0.8, while gels incubated at pH 13 yielded 0.1 after 5 h and 0.01 after 1 day.

Acknowledgements

This work was supported by VISTA (grant V6312), a research cooperation between the Norwegian Academy of Science and Letters, and Statoil. We gratefully acknowledge Sanofi Bioindustries, France for providing the scleroglucan sample.

References

Aasprong, E., Smidsrød, O., & Stokke, B. T. (2003). Scleroglucan gelation by in situ neutralization of the alkaline solution. *Biomacromolecules*, *4*, 914–921.

Becker, N., Oroudjev, E., Mutz, S., Cleveland, J. P., Hansma, P. K., Hayashi, C. Y., et al. (2003). Molecular nanosprings in spider capture-silk threads. *Nature Materials*, *2*, 278–283.

Blatz, P. J., Sharda, S. C., & Tschoegl, N. W. (1974). Strain energy function for rubber-like materials based on a generalized measure of strain. *Transactions of the Society of Rheology*, *18*, 145–161.

Bluhm, T. L., Deslandes, Y., & Marchessault, R. H. (1982). Solid-state and solution conformation of scleroglucan. *Carbohydrate Research*, *100*, 117–129.

Bo, S., Milas, M., & Rinaudo, M. (1987). Behaviour of scleroglucan in aqueous solution containing sodium hydroxide. *International Journal of Biological Macromolecules*, *9*, 153–157.

Bohn, J. A., & BeMiller, J. N. (1995). (1→3)-β-D-glucans as biological response modifiers: a review of structure–functional activity relationships. *Carbohydrate Polymers*, *28*, 3–14.

Bot, A., van Amerongen, I. A., Groot, R. D., Hoekstra, N. L., & Agterof, W. G. M. (1996). Large deformation rheology of gelatin gels. *Polymer Gels and Networks*, *4*, 189–227.

Carriere, C. J., Amis, E. J., Schrag, J. L., & Ferry, J. D. (1985). Dilute-solution dynamic viscoelastic properties of schizophyllan polysaccharide. *Macromolecules*, *18*, 2019–2023.

Clark, A. H., & Ross-Murphy, S. B. (1987). Structural and mechanical properties of biopolymer gels. *Advances in Polymer Science*, *83*, 57–192.

Coviello, T., Grassi, M., Rambone, G., & Alhaique, F. (2001). A crosslinked system from Scleroglucan derivative: Preparation and characterization. *Biomaterials*, *22*, 1899–1909.

Dubois, M., Gilles, K. A., Hamilton, J. K., Rebers, P. A., & Smith, F. (1956). Colorimetric method for determination of sugars and related substances. *Analytical Chemistry*, *28*, 350–356.

Falch, B. H., Elgsaeter, A., & Stokke, B. T. (1999). Exploring the (1→3)-β-D-glucan conformational phase diagrams to optimize the linear to macrocycle conversion of the triple-helical polysaccharide scleroglucan. *Biopolymers*, *50*, 496–512.

Falch, B. H., & Stokke, B. T. (2001). Structural stability of (1→3)-β-D-glucan macrocycles. *Carbohydrate Polymers*, *44*, 113–121.

Ferry, J. D. (1980). *Viscoelastic properties of polymers*. USA: Wiley.

Flynn, K. J. (1988). Some practical aspects of measurements of dissolved free amino acids in natural waters and within microalgae by the use of HPLC. *Chemistry and Ecology*, *3*, 269–293.

Fung, Y. C. B. (1967). Elasticity of soft tissues in simple elongation. *American Journal of Physiology*, *213*, 1532.

Groot, R. D., Bot, A., & Agterof, W. G. M. (1996). Molecular theory of strain hardening of a polymer gel: Application to gelatin. *Journal of Chemical Physics*, *104*, 9202–9219.

Guo, B., Elgsaeter, A., Christensen, B. E., & Stokke, B. T. (1998). Scleroxchitosan co-gels: Effects of charge density on swelling of gels in ionic aqueous solution and in poor solvents, and on the rehydration of dried gels. *Polymer Gels and Networks*, *6*, 471–492.

Hjerde, T., Stokke, B. T., Smidsrød, O., & Christensen, B. E. (1998). Free-radical degradation of triple-stranded scleroglucan by hydrogen peroxide and ferrous ions. *Carbohydrate Polymers*, *37*, 41–48.

Itou, T., Teramoto, A., Matsua, T., & Suga, H. (1986). Ordered structure in aqueous polysaccaride. 5. Cooperative order–disorder transition in aqueous schizophyllan. *Macromolecules*, *19*, 1234–1240.

Itou, T., Teramoto, A., Matsua, T., & Suga, H. (1987). Isotope effect on the order–disorder transition in aqueous schizophyllan. *Carbohydrate Research*, *160*, 243–257.

Johnson, J., Kirkwood, S., Misaki, A., Nelson, T. E., Scaletti, J. V., & Smith, F. (1963). Structure of a new glucan. *Chemistry and Industry* , 820–822.

Kalpacki, B., Jeans, Y. T., Magri, N. F., & Padolewski, J. P. (1990). Thermal stability of scleroglucan at realistic reservoir conditions. *Society of Petroleum Engineers* , 602–613.

Kirsten, W. J. (1979). Automatic methods for the simultaneous determination of carbon, hydrogen, nitrogen, and sulfur, and for sulfur alone in organic and inorganic materials. *Analytical Chemistry*, *51*, 1173–1179.

Kitamura, S., Hirano, T., Takeo, K., Fukada, H., Takahashi, K., Falch, B. H., et al. (1996). Conformational transitions of schizophyllan in aqueous alkaline solution. *Biopolymers*, *39*, 407–416.

Kitamura, S., & Kuge, T. (1989). A differential scanning calorimetric study of the conformational transitions of schizophyllan in mixtures of water and dimethylsulfoxide. *Biopolymers*, *28*, 639–654.

Kojima, T., Tabata, K., Itoh, W., & Yanaki, T. (1986). Molecular weight dependence of the antitumor activity of schizophyllan. *Agricultural and Biological Chemistry*, *50*, 231–232.

Konno, A., & Harada, T. (1991). Thermal-properties of curdlan in aqueous suspension and curdlan gel. *Food Hydrocolloids*, *5*, 427–434.

Lindroth, P., & Mopper, K. (1979). High performance liquid chromatographic determination of subpicomole amounts of amino acids by precolumn fluorescence derivatization with *o*-phthaldialdehyde. *Analytical Chemistry*, *51*, 1667–1674.

Lowry, O. H., Rosebrough, N. J., Farr, A. L., & Randall, R. J. (1951). Protein measurement with the folin phenol reagent. *Journal of Biological Chemistry*, *193*, 265–275.

Mohaček-Grošev, V., Božac, R., & Puppels, G. J. (2001). Vibrational spectroscopic characterization of wild growing mushrooms and toadstools. *Spectrochimica Acta. Part A. Molecular Spectroscopy*, *57*, 2815–2829.

Palace, G. P., & Phoebe, C. H. (1997). Quantitative determination of amino acid levels in neutral and glucosamine-containing carbohydrate polymers. *Analytical Biochemistry*, *244*, 393–403.

Peterson, G. L. (1979). Review of the folin phenol protein quantitation method of Lowry. Rosebrough, Farr and Randall. *Analytical Biochemistry*, *100*, 201–220.

Rouse, P. E. (1953). A theory of the linear viscoelastic properties of dilute solutions of coiling polymers. *Journal of Chemical Physics*, *21*, 1272–1280.

Sato, T., Norisuye, T., & Fujita, H. (1981). Melting behavior of shizophyllum commune polysaccharides in mixtures of water and dimethyl sulfoxide. *Carbohydrate Research*, *95*, 195–204.

Stokke, B. T., & Brant, D. A. (1990). The reliability of wormlike polysaccharide chain dimensions estimated from electron micrographs. *Biopolymers*, *30*, 1161–1181.

Stokke, B. T., Elgsaeter, A., & Kitamura, S. (1993). Macrocyclization of polysaccharides visualized by electron microscopy. *International Journal of Biological Macromolecules*, *15*, 63–68.

Stokke, B. T., Elgsaeter, A., Smidsrød, O., & Christensen, B. E. (1995). Carboxylation of scleroglucan for controlled crosslinking by heavy metal ions. *Carbohydrate Polymers*, *27*, 5–11.

Treloar, L. R. G. (1975). *The physics of rubber elasticity* (3rd ed.). Oxford: Clarendon Press.

Wasser, S. P. (2002). Medicinal mushrooms as a source of antitumor and immunomodulating polysaccharides. *Applied Microbiology and Biotechnology*, *60*, 258–274.

Yanaki, T., Norisuye, T., & Fujita, H. (1980). Triple helix of schizophyllum-commune polysaccharide in dilute solution. 3. Hydrodynamic properties in water. *Macromolecules*, *13*, 1462–1466.

Yanaki, T., Tabata, K., & Kojima, T. (1985). Melting behaviour of a triple helical polysaccharide schizophyllan in aqueous solution. *Carbohydrate Polymers*, *5*, 275–283.

Zhang, H., Nishinari, K., Williams, M. A. K., Foster, T. J., & Norton, I. T. (2002). A molecular description of the gelation mechanism of curdlan. *International Journal of Biological Macromolecules*, *30*, 7–16.